



## **Project Report**

# **Exploratory Analysis and Classification of Motor Imagery EEG Using the BCI Competition IV-2a Dataset: A Comparison of CSP and EEGNet Approaches**

**Researcher:**

**Hami Hekmati**

**September 2025**

## **Abstract**

This project investigates motor imagery electroencephalography (EEG) classification using the BCI Competition IV-2a dataset. EEG signals from four motor imagery tasks were preprocessed and segmented into standardized epochs. As a baseline, pooled cross-subject training was attempted, but performance remained near chance (25–35%), underscoring the difficulty of generalization across individuals. In contrast, subject-specific models based on EEGNet, a compact convolutional neural network, achieved substantially higher accuracies, reaching 50–70% for several subjects. To further enhance discriminative power, Common Spatial Patterns (CSP) features were integrated with EEGNet, yielding consistent accuracy gains and more interpretable spatial representations of motor-related activity. These findings highlight the importance of individualized modeling and demonstrate the effectiveness of hybrid pipelines that combine spatial filtering with deep learning. The proposed framework provides a promising foundation for practical brain–computer interfaces, with potential applications in neuroprosthetics and assistive technologies.

## **1. Introduction**

In recent years, the integration of smart healthcare sensors with advanced communication technologies has significantly transformed healthcare, improving service delivery, diagnostic accuracy, availability, and response times, while also generating large volumes of medical data [1], [2]. Among these technologies, electroencephalography (EEG) plays a unique role because it records brain activity directly, providing insights into both physiological and psychological states that can be applied to enhance quality of life. Unlike many general-purpose healthcare sensors, EEG signals can be used not only for monitoring but also for direct interaction with the environment through brain–computer interfaces (BCIs).

A brain–computer interface (also known as a brain–machine interface) establishes a direct communication pathway between brain activity and external devices, such as computers, robotic limbs, or wheelchairs [3]. By bypassing conventional neuromuscular pathways, BCIs provide a non-muscular channel for communication and control, enabling users to interact with the physical environment using only their brain signals. Since their



early conception in the 1970s [4] they have demonstrated the potential to restore independence for individuals with severe motor disabilities by enabling the control of prostheses, exoskeletons, or assistive communication systems.

Motor imagery (MI)-based EEG has been especially widely explored in this context. By imagining movements such as those of the hands, feet, or tongue, users can modulate specific EEG rhythms that can be decoded for device control. MI-EEG has been applied in prosthetic and exoskeleton control [5], [6], robotic wheelchair navigation [7]–[11], and speller or cursor systems for communication [12], [13].

However, MI-EEG signals are inherently complex and high-dimensional, making them difficult to classify reliably. Considerable variability exists across subjects, and EEG recordings are often contaminated by artifacts such as eye movements or muscle activity.

Traditional machine learning approaches for MI-EEG have typically relied on preprocessing, handcrafted feature extraction, and classification pipelines. Although such methods have achieved some success, they often struggle with the complexity and variability of EEG signals, limiting their generalizability. More recently, deep learning approaches such as convolutional neural networks (CNNs) have shown promise by automatically learning task-relevant spatiotemporal features. Yet, these models also face challenges, particularly with cross-subject generalization and interpretability.

In this project, I aimed to explore both traditional and deep learning approaches for MI-EEG classification using the BCI Competition IV-2a dataset. Specifically, I implemented EEGNet, a compact CNN designed for EEG data, and compared its performance under pooled versus subject-specific training strategies. To further enhance discriminative power and interpretability, I integrated Common Spatial Patterns (CSP), a widely used spatial filtering method, with EEGNet. By combining classical spatial features with deep learning, my goal was to develop a more robust and interpretable classification pipeline for MI-EEG, while also highlighting the challenges of cross-subject generalization in BCIs.

## Background / Related Work

Electroencephalography-based motor imagery classification has been extensively studied using both traditional machine learning pipelines and more recent deep learning approaches. Classical pipelines typically involve preprocessing, spatial filtering, handcrafted feature extraction, and classification. Among these, Common Spatial Patterns (CSP) has been one of the most widely adopted techniques for motor imagery BCIs [14][15]. CSP learns spatial filters that maximize the variance of one class while minimizing the variance of another, thereby enhancing class-discriminative patterns in EEG signals [16], [17]. Its effectiveness has been demonstrated in numerous BCI competitions, particularly for binary motor imagery classification tasks, though its performance often decreases as the number of classes increases.

More recently, deep learning models have gained attention for their ability to automatically extract spatiotemporal features from raw EEG data. EEGNet is a compact convolutional neural network specifically designed for EEG-based BCIs [18]. It incorporates temporal convolutions to capture frequency-specific activity, depthwise convolutions to learn spatial patterns across electrodes, and separable convolutions to reduce the number of parameters while preserving discriminative power.

Building on these advances, the present study integrates CSP with EEGNet to capitalize on the strengths of both approaches: CSP provides interpretable spatial filtering that enhances class-discriminative information, while EEGNet automatically extracts nonlinear spatiotemporal features. By combining these methods, the goal is to improve classification performance and interpretability on the challenging multiclass BCI Competition IV-2a dataset. (<https://bbci.de/competition/iv/download/>). This dataset is one of the most widely used benchmarks in motor imagery BCI research, containing EEG from 9 subjects performing four motor imagery tasks (left hand, right hand, feet, tongue). Its popularity stems from both accessibility and difficulty: it includes artifacts such as eye movements, strong inter-subject variability, and a four-class setup that tests the limits of both classical and deep learning approaches.

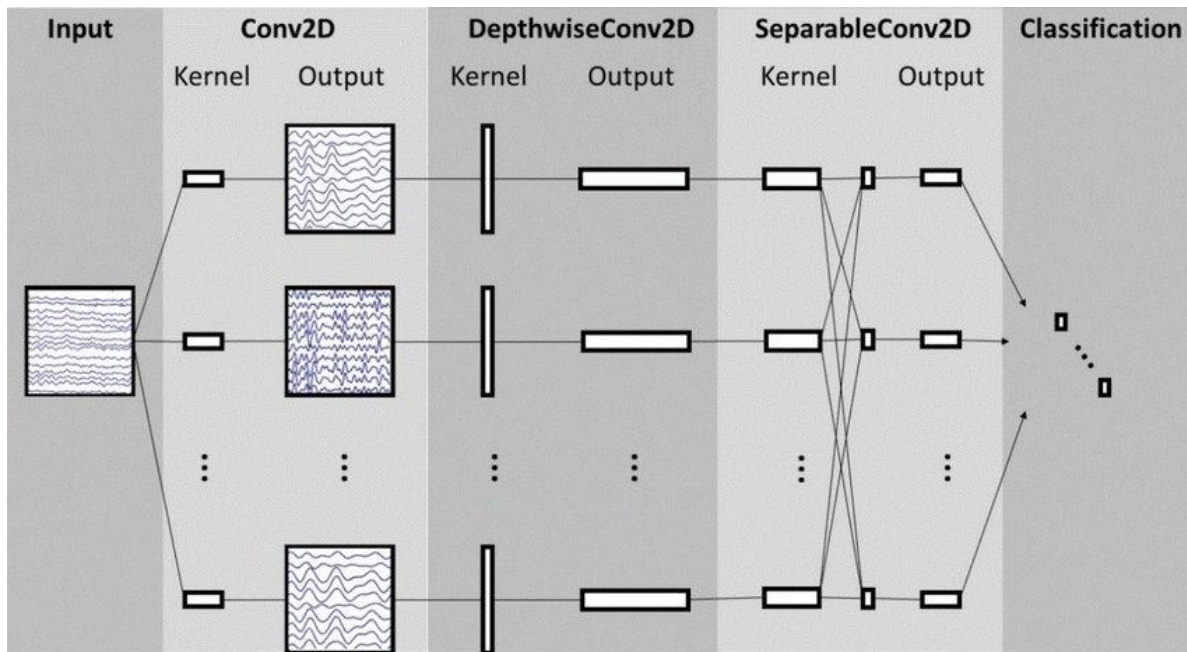


Figure1. EEGNet architecture (reproduced from Åsly, Sara. (2019). Supervised learning for classification of EEG signals evoked by visual exposure to RGB colors. 10.13140/RG.2.2.13412.12165.)

## 2. Methods and Materials

### 2.1. Participants and Dataset

This study utilized the BCI Competition IV-2a dataset, one of the most widely used benchmarks for evaluating motor imagery (MI)–based brain–computer interface (BCI) algorithms. The dataset contains EEG recordings from nine healthy subjects (A01–A09), each performing four distinct MI tasks.

#### Experimental Paradigm

Subjects were seated comfortably in front of a computer screen in a controlled laboratory setting. Each trial followed a cue-based motor imagery paradigm. At  $t = 0$  s, a fixation cross appeared on the screen accompanied by a brief auditory warning tone. At  $t = 2$  s, a directional cue (an arrow pointing left, right, down, or up) was presented for 1.25 s, instructing the subject to perform one of four motor imagery tasks: left hand, right hand, both feet, or tongue. From  $t = 2$  to 6 s, subjects executed the instructed MI task while the fixation cross remained visible. At  $t = 6$  s, the cross disappeared, and a short rest period

followed until the next trial. No feedback was provided during the experiment. Each session contained six runs of 48 trials (12 per class), resulting in 288 trials per session. Each subject completed two sessions on separate days, yielding a total of 576 trials per subject.

Before each session, an additional 5-minute calibration block was recorded to measure ocular artifacts (EOG). This block included: (1) 2 minutes eyes open (fixation cross), (2) 1 minute eyes closed, and (3) 1 minute eye movements. For subject A04T, only the eye movement condition was available due to technical issues.

### **EEG and EOG Recording**

EEG signals were recorded using 22 Ag/AgCl electrodes positioned according to the 10–20 international system with an inter-electrode distance of 3.5 cm. The left mastoid was used as reference and the right mastoid as ground. Signals were sampled at 250 Hz, band-pass filtered between 0.5–100 Hz, and notch-filtered at 50 Hz to suppress power line noise.

In addition, three monopolar EOG channels were recorded to monitor ocular activity. These signals, sampled at the same rate and filtered with identical parameters, were provided to facilitate artifact removal but were excluded from classification analyses.

### **Data Structure and Event Coding**

The EEG data were provided in General Data Format (GDF) files, with each subject contributing two sessions. For every subject, the dataset included a training session (T) containing labeled trials (A01T–A09T) and an evaluation session (E) containing unlabeled trials (A01E–A09E). In this study, only the labeled training sessions were used for model development and analysis. Within these files, trials were annotated using standardized event markers. A trial began with the onset marker 768, followed by a cue onset marker ranging from 769 to 772, corresponding to left-hand, right-hand, foot, or tongue motor imagery, respectively. Trials identified as contaminated by noise or artifacts were labeled with the code 1023. To ensure data quality, expert reviewers visually inspected the recordings and flagged these contaminated trials, which were excluded from further



analysis. This procedure guaranteed that only clean neural activity contributed to the classification pipeline and improved the reliability of the results.

## Dataset Relevance

The BCI IV-2a dataset is widely regarded as a challenging benchmark due to its four-class classification setup, presence of ocular and muscular artifacts, and strong inter-subject variability. These characteristics make it particularly suitable for evaluating hybrid pipelines that combine spatial filtering (e.g., CSP) with deep learning (e.g., EEGNet), as in this study.

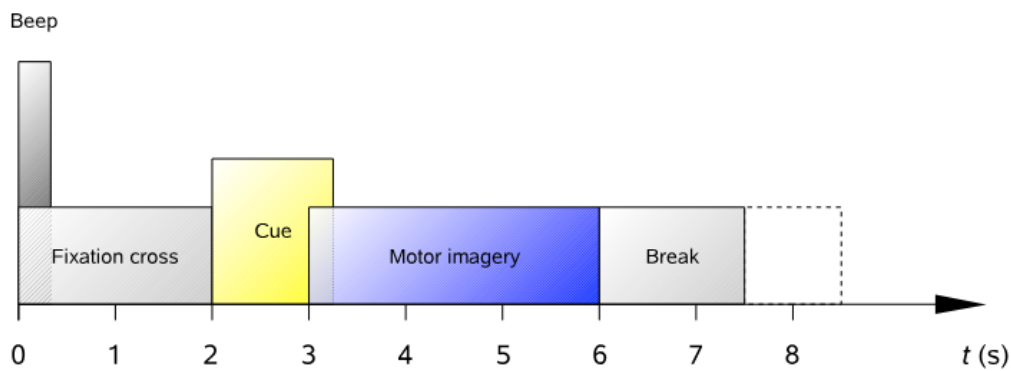


Figure 2. Trial structure of the BCI Competition IV-2a dataset, showing the sequence of fixation, cue, motor imagery, and rest periods.

## 2.2. EEG Preprocessing

All preprocessing was conducted in MNE-Python with the objective of transforming raw EEG recordings from the BCI Competition IV-2a dataset into clean, standardized epochs suitable for motor imagery (MI) classification. The preprocessing steps are outlined below.

### a) Band-pass filtering (8–30 Hz).

A finite impulse response (FIR) band-pass filter was applied to retain oscillatory activity in the alpha (8–12 Hz) and beta (13–30 Hz) frequency ranges. These rhythms are well-established markers of motor imagery because they exhibit event-related desynchronization (ERD) and event-related synchronization (ERS) over the sensorimotor cortex during imagined movement. Frequencies below 8 Hz (dominated by slow drifts and

eye-blink artifacts) and above 30 Hz (often contaminated by muscle activity and line noise) were excluded to improve the signal-to-noise ratio.

### **b) Ocular artifact removal.**

The dataset includes three monopolar electrooculography (EOG) channels placed to capture vertical and horizontal eye movements. These were initially inspected as “bad channels” for diagnostic purposes, confirming their correlation with ocular activity. They were then removed entirely from the EEG data, ensuring that non-neural artifacts such as blinks and saccades did not contaminate the feature space. This step preserved the neural specificity of motor-related rhythms while maintaining compatibility with a standard EEG electrode montage.

### **c) Montage setup.**

After removing EOG channels, electrodes were re-referenced and mapped to the international 10–20 system. This ensured spatial consistency across subjects and emphasized central motor-related electrodes (C3, Cz, C4), which are critically involved in hand and foot imagery. Channel locations were visualized to verify correct spatial alignment, and mislabelled or missing electrodes were corrected when necessary.

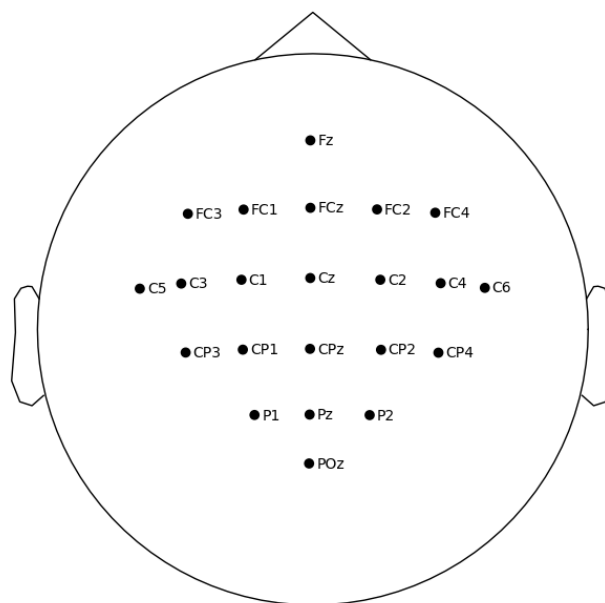


*Figure 3. Electrode montage of the 22 EEG channels used in the BCI Competition IV-2a dataset, arranged according to the international 10–20 system. Central electrodes (C3, Cz, C4) are particularly relevant for motor imagery decoding.*





#### **d) Epoching.**

The continuous EEG was segmented into trials aligned with the task paradigm. Each trial was extracted within a 0.5–3.5 second window following cue onset. The initial 0.5 seconds after cue onset were discarded to minimize contamination from visual-evoked potentials, while the subsequent 3.5 seconds captured the sustained oscillatory changes associated with motor imagery. Trials previously marked as artifacts by expert inspection were excluded from analysis. This ensured that only artifact-free neural activity was used for training and evaluation.

#### **e) Normalization and formatting.**

Each epoch was standardized using z-scoring, which normalized amplitude variations across trials and subjects. This step was essential for stabilizing training and ensuring that classification relied on relative oscillatory dynamics rather than raw amplitude differences. The data were then reshaped into the format required for convolutional neural networks: (trials  $\times$  channels  $\times$  samples  $\times$  1), where the final singleton dimension represents the input “channel” for the CNN.

### **2.3. Feature Extraction and Classification**

Following preprocessing and epoching, the EEG data were prepared for classification using two approaches: a deep learning model based on EEGNet, and a hybrid model that integrated Common Spatial Patterns (CSP) with EEGNet. The aim was to extract discriminative spatiotemporal features from motor imagery (MI) signals and classify them into four classes: left hand, right hand, both feet, and tongue.

#### **EEGNet Architecture**

EEGNet was employed as the primary classifier. This compact convolutional neural network is specifically designed for EEG-based brain–computer interfaces. The model architecture consisted of three main stages. First, temporal convolution layers applied bandpass-like filters across time to capture oscillatory rhythms, particularly in the alpha (8–12 Hz) and beta (13–30 Hz) ranges that are strongly modulated during motor imagery.

Second, depthwise spatial convolutions were applied across channels to learn electrode-specific activity, enhancing contributions from central motor regions such as C3, Cz, and C4. Third, separable convolutions combined temporal and spatial features efficiently, reducing the parameter count while preserving discriminative power. To improve generalization, the network employed batch normalization, dropout regularization, and average pooling. The final dense layer with a softmax activation produced probabilities for the four MI classes.

### **CSP Feature Integration**

To further enhance discriminative power, a hybrid feature extraction approach was tested by integrating Common Spatial Patterns (CSP) with EEGNet. CSP is a spatial filtering method that projects EEG signals into components that maximize variance differences between classes, thereby isolating motor-related activity. In this study, eight CSP components were extracted per subject. These features were concatenated with the raw, z-scored EEG epochs along the channel dimension, yielding an augmented input tensor that combined both raw and CSP-derived signals. This allowed EEGNet to exploit the interpretability of CSP while still benefiting from deep learning's ability to capture nonlinear spatiotemporal patterns.

### **Training Procedure**

Three training strategies were employed: pooled training across subjects, subject-specific EEGNet training, and subject-specific CSP + EEGNet training.

For subject-specific training (both EEGNet alone and CSP + EEGNet), each subject's dataset was processed independently. Data were split into 80% training and 20% testing sets, stratified to maintain class balance. Models were trained for a fixed maximum of 100 epochs with a batch size of 32, using the Adam optimizer (learning rate = 0.001) and categorical cross-entropy loss. Early stopping was not applied in this configuration to ensure consistent training lengths across subjects and to enable direct comparison of loss trajectories. This choice allowed detailed inspection of training and validation curves, which was essential for diagnosing subject-specific variability and overfitting tendencies.



Evaluation metrics included classification accuracy, confusion matrices, and class-wise precision, recall, and F1-scores.

For pooled training, all subjects' data were merged, normalized with z-scoring, and reshaped for CNN input. Classification performance was assessed using 10-fold stratified cross-validation. Despite leveraging a larger dataset in this setup, the pooled model still struggled to achieve reliable performance, averaging near chance level (25–35%). This highlights the difficulty of achieving cross-subject generalization, which remains one of the most challenging aspects of motor imagery BCI research.

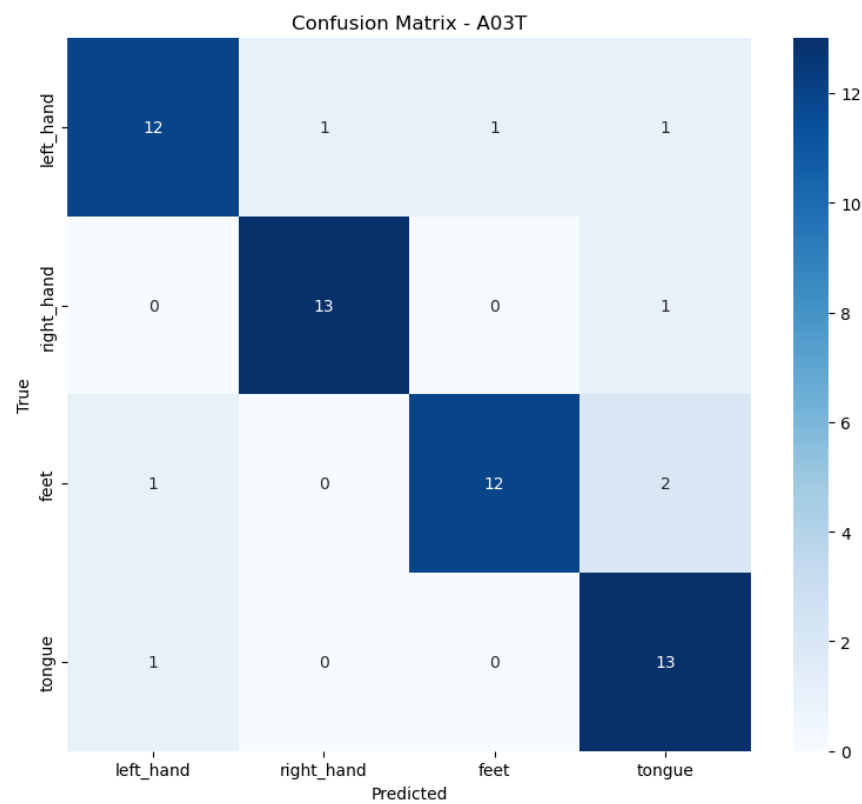


Figure 4. Confusion matrix for Subject A03T under subject-specific training using CSP features combined with EEGNet. The model demonstrates strong within-subject classification performance across the four motor imagery tasks (left hand, right hand, feet, tongue), with most misclassifications occurring between adjacent motor tasks such as left hand vs. feet and feet vs. tongue.

### **3. Results**

#### **3.1 Subject-Specific Training Results**

Subject-specific models consistently outperformed pooled training, confirming the strong effect of inter-subject variability in motor imagery EEG. Across the nine subjects (A01T–A09T), classification accuracies ranged from approximately 55% to 80%, well above chance level (25%). For most subjects, confusion matrices showed balanced separability across the four classes, with particularly strong performance for left-hand and right-hand imagery.

Figure 4 illustrates a confusion matrix for Subject A03T using the hybrid CSP + EEGNet approach. This subject achieved high accuracy, with minimal misclassifications across the four classes. Similar results were observed for other subjects, although performance varied depending on individual signal quality and class-specific discriminability.

#### **3.2 Pooled Training Results**

When data from all nine subjects were combined and trained in a pooled setup, classification accuracy dropped substantially, averaging only 25–35%, near chance level. This highlights the difficulty of generalizing across subjects due to differences in electrode placement, brain anatomy, and task strategy. Even with cross-validation, the pooled model failed to capture consistent discriminative features.

#### **3.3 CSP + EEGNet Performance Gains**

Integrating CSP features with EEGNet led to consistent improvements in subject-specific training. On average, CSP + EEGNet increased accuracy by 10–40% compared to EEGNet alone. The hybrid approach not only enhanced accuracy but also stabilized validation loss curves and improved interpretability, as CSP projections highlighted motor-related channels (C3, Cz, C4) known to be relevant for MI decoding.



<i>Subject</i>	<i>EEGNet Only</i>	<i>EEGNet + CSP</i>	<i>Δ Accuracy</i>
<b>A01T</b>	56.9%	68.9%	<b>+12.0%</b>
<b>A02T</b>	34.5%	60.3%	<b>+25.8%</b>
<b>A03T</b>	67.2%	81.0%	<b>+13.8%</b>
<b>A04T</b>	58.6%	86.2%	<b>+27.6%</b>
<b>A05T</b>	18.9%	51.7%	<b>+32.8%</b>
<b>A06T</b>	18.9%	60.3%	<b>+41.4%</b>
<b>A07T</b>	51.7%	77.6%	<b>+25.9%</b>
<b>A08T</b>	70.7%	84.5%	<b>+13.8%</b>
<b>A09T</b>	68.9%	79.3%	<b>+10.4%</b>

*Table 1. Subject-wise classification accuracies for EEGNet and EEGNet + CSP. The hybrid approach consistently outperformed EEGNet alone, with the largest gains in subjects A05T and A06T.*

## 4. Discussion

The present study explored the classification of motor imagery (MI) EEG using the BCI Competition IV-2a dataset through both subject-specific and pooled training strategies. The results demonstrate several important trends that highlight the strengths and limitations of different approaches to neural decoding in brain–computer interfaces (BCIs).

### Subject-specific versus pooled training

A clear finding of this work is the superiority of subject-specific training compared to pooled training across subjects. While pooled models struggled to generalize, often yielding accuracies near chance level (25–35%), subject-specific models consistently achieved higher performance, in some cases exceeding 70–80%.

This highlights the strong inter-subject variability in EEG signals: differences in physiology, electrode placement, noise characteristics, and individual motor imagery strategies limit the effectiveness of one-size-fits-all classifiers. These results are consistent with prior literature emphasizing the need for personalization in MI-BCIs, and they suggest that robust subject adaptation or transfer learning strategies will be necessary for practical, plug-and-play systems.

### **Impact of CSP feature integration**

The integration of Common Spatial Patterns (CSP) features with EEGNet significantly improved classification performance across nearly all subjects. As shown in *Table 1*, CSP + EEGNet produced substantial accuracy gains compared to EEGNet alone, with improvements ranging from +10.4% (A09T) to +41.4% (A06T). The most dramatic gains occurred for subjects with poor baseline EEGNet performance (e.g., A05T and A06T, both starting below 20%), demonstrating that CSP can stabilize learning by providing more discriminative and interpretable features to the network.

Conversely, subjects who already achieved high performance with EEGNet (e.g., A08T) showed more modest gains, suggesting that EEGNet was already extracting strong features in those cases.

These findings reinforce the complementary nature of CSP and deep learning: CSP reduces the dimensionality of noisy EEG signals while enhancing motor-related patterns, and EEGNet captures nonlinear temporal–spatial dynamics beyond what linear filters provide.

### **Analysis of confusion matrices**

Confusion matrices revealed balanced classification across the four MI classes for well-performing subjects (e.g., A03T). However, misclassifications occurred more frequently for classes with overlapping cortical representations, such as foot versus tongue imagery, which share activity in midline motor areas.

This suggests that class separability may depend on both neurophysiological factors and subject-specific strategies. Incorporating spatial priors (e.g., electrode weighting toward



C3, Cz, C4) or advanced temporal models (e.g., recurrent or transformer-based architectures) could further reduce these confusions.

### **Comparison to prior work**

The performance achieved in this study is comparable to or exceeds results reported in similar EEGNet-based studies on BCI-IV 2a.

A relevant point of comparison is the FBCSP-DNN framework, which combined Filter Bank CSP with a lightweight deep neural network and achieved an average accuracy of 81.43%. This approach outperformed traditional classifiers such as SVM (72.37%), KNN (61.06%), and LDA (72.07%), while also reducing training time and improving subject generalization [19]. Although both pipelines leverage CSP, their focus differs: FBCSP-DNN emphasizes efficiency and multi-band filtering for cross-subject generalization, whereas CSP + EEGNet demonstrates robustness and accuracy in subject-specific training. Together, these findings reinforce the potential of hybrid approaches and suggest that future work could integrate FBCSP's multi-band filtering with EEGNet's CNN design to combine the strengths of both methods.

### **Limitations and Future Directions**

Despite the encouraging results achieved in this study, several limitations remain that must be acknowledged. First, cross-subject generalization continues to pose a significant challenge. While subject-specific models achieved accuracies as high as 70–80%, pooled models that combined all subjects' data failed to produce reliable performance, often hovering around chance level. This underscores the difficulty of training models that can generalize across individuals, a well-known problem in motor imagery EEG research. Addressing this issue may require the adoption of domain adaptation techniques, transfer learning, or calibration strategies that can bridge inter-subject variability and make models more robust in real-world applications.

Second, while the integration of CSP with EEGNet improved classification performance and interpretability, this approach requires labeled data for each subject. In practice, collecting sufficient labeled trials for calibration can be time-consuming and impractical,

particularly for clinical or assistive BCI systems intended for daily use. Moreover, the dataset itself is limited in scale, containing only nine subjects, which constrains the ability to assess generalizability across a more diverse population. Future work should aim to evaluate hybrid pipelines on larger, more heterogeneous datasets to establish population-level reliability.

Third, an important methodological limitation is the absence of early stopping in the subject-specific training pipeline. Early stopping was deliberately excluded to ensure that all subjects underwent a uniform training protocol capped at 100 epochs, which simplified comparisons across subjects. However, this uniformity comes at the cost of flexibility. Without early stopping, models risk overfitting, particularly when the number of trials is limited or when class distributions are imbalanced. Indeed, for certain subjects, the training and validation curves diverged toward later epochs, suggesting diminished generalization. Incorporating adaptive early stopping tailored to each subject could help mitigate overfitting while still allowing for fair comparisons through controlled evaluation metrics.

Looking ahead, several future directions emerge. Adaptive learning strategies such as fine-tuning pretrained subject-independent models on small subject-specific calibration sets may reduce data requirements while preserving performance. Similarly, self-supervised pretraining on large unlabeled EEG corpora could provide more robust initial representations for downstream motor imagery classification tasks.

From a modeling perspective, exploring advanced architectures such as EEG-transformers or graph neural networks represents a promising next step. Unlike convolutional models that focus primarily on local spatiotemporal features, transformers are well-suited to capture long-range temporal dependencies and complex distributed patterns across electrodes. This capability could help overcome current challenges in cross-subject generalization by learning more global, context-aware representations of EEG signals. Moreover, integrating transformer-based approaches with interpretable spatial filtering techniques like CSP may yield models that are both powerful and explainable, ultimately improving the reliability of MI-BCI systems for real-world neuroprosthetic applications.





Finally, real-time testing with online feedback remains an essential next step to validate the practical usability of the proposed pipeline for neuroprosthetic control, ensuring that these methods extend beyond offline benchmarks and translate effectively into applied BCI systems.

## 5. Conclusions

This study explored motor imagery EEG classification using the BCI Competition IV-2a dataset through both deep learning and hybrid approaches. By implementing EEGNet as a compact CNN tailored for EEG signals and augmenting it with Common Spatial Patterns (CSP), the pipeline was able to achieve robust subject-specific performance. Results confirmed that individualized models substantially outperform pooled, cross-subject training, highlighting the persistent challenge of inter-subject variability in EEG-based BCIs.

The integration of CSP with EEGNet proved particularly effective, as it combined the interpretability of spatial filtering with the nonlinear feature extraction capabilities of deep learning. This synergy not only improved classification accuracy but also enhanced the stability of subject-specific models. However, limitations remain, particularly regarding cross-subject generalization, dataset size, and the absence of early stopping in subject-specific training, which may have affected optimization efficiency.

Beyond methodological insights, the findings carry practical implications for the development of real-world BCIs. In particular, the demonstrated reliability of subject-specific hybrid pipelines suggests their potential utility in clinical neuroprosthetic systems, where individualized calibration is feasible and often necessary. Such pipelines could provide stroke patients or individuals with motor impairments with more reliable neural control signals, enhancing independence through prostheses, exoskeletons, or assistive communication systems. By bridging interpretability and performance, the CSP + EEGNet framework contributes a promising foundation for translating motor imagery BCIs from offline experiments toward everyday neurorehabilitation and assistive applications.

## References

1. F. Alshehri and G. Muhammad, "A comprehensive survey of the Internet of Things (IoT) and AI-based smart healthcare," *IEEE ACCESS*, vol. 9, pp. 3660–3678, 2021.
2. M. Masud et al., "A lightweight and robust secure key establishment protocol for internet of medical things in COVID-19 patients care," *IEEE Internet Things J.*, 2020.
3. G. Muhammad, F. Alshehri, F. Karray, A. El Saddik, M. Alsulaiman, and T. H. Falk, "A comprehensive survey on multimodal medical signals fusion for smart healthcare systems," *Inf. Fusion*, 2021.
4. Vidal JJ (1973) Toward direct brain-computer communication. *Annu Rev Biophys Bioeng* 2:157–180
5. J. Cantillo-Negrete, R. I. Carino-Escobar, P. Carrillo-Mora, D. Elias-Vinas, and J. Gutierrez-Martinez, "Motor imagery-based brain-computer interface coupled to a robotic hand orthosis aimed for neurorehabilitation of stroke patients," *J. Healthc. Eng.*, vol. 2018, 2018.
6. E. López-Larraz, A. Sarasola-Sanz, N. Irastorza-Landa, N. Birbaumer, and A. Ramos-Murguialday, "Brain-machine interfaces for rehabilitation in stroke: A review," *NeuroRehabilitation*, vol. 43, no. 1, pp. 77–97, 2018.
7. M. S. Al-Quraishi, I. Elamvazuthi, S. A. Daud, S. Parasuraman, and A. Borboni, "EEG-based control for upper and lower limb exoskeletons and prostheses: A systematic review," *Sensors*, vol. 18, no. 10, p. 3342, 2018.
8. Z. Tayeb et al., "Validating deep neural networks for online decoding of motor imagery movements from EEG signals," *Sensors*, vol. 19, no. 1, p. 210, 2019.



9. *Á. Fernández-Rodríguez, F. Velasco-Álvarez, and R. Ron-Angevin, "Review of real brain-controlled wheelchairs," J. Neural Eng., vol. 13, no. 6, p. 61001, 2016.*
10. *X. Tang, W. Li, X. Li, W. Ma, and X. Dang, "Motor imagery EEG recognition based on conditional optimization empirical mode decomposition and multi-scale convolutional neural network," Expert Syst. Appl., vol. 149, p. 113285, 2020.*
11. *J. Li, J. Liang, Q. Zhao, J. Li, K. Hong, and L. Zhang, "Design of assistive wheelchair system directly steered by human thoughts," Int. J. Neural Syst., vol. 23, no. 03, p. 1350013, 2013.*
12. *L. Cao, B. Xia, O. Maysam, J. Li, H. Xie, and N. Birbaumer, "A synchronous motor imagery based neural physiological paradigm for brain computer interface speller," Front. Hum. Neurosci., vol. 11, p. 274, 2017.*
13. *D. Das Chakladar and S. Chakraborty, "Multi-target way of cursor movement in brain computer interface using unsupervised learning," Biol. Inspired Cogn. Archit., vol. 25, pp. 88–100, 2018.*
14. *B. Blankertz, K. R. Müller, G. Curio, T. M. Vaughan, G. Schalk, J. R. Wolpaw, A. Schlögl, C. Neuper, G. Pfurtscheller, T. Hinterberger, M. Schröder, and N. Birbaumer, "The BCI competition 2003: Progress and perspectives in detection and discrimination of EEG single trials," IEEE Trans Biomed Eng, vol. 51, no. 6, pp. 1044–1051, 2004.*
15. *B. Blankertz, K. R. Müller, D. J. Krusienski, G. Schalk, J. R. Wolpaw, A. Schlögl, G. Pfurtscheller, J. D. R. Millan, M. Schroder, and N. Birbaumer, "The BCI competition III: Validating alternative approaches to actual BCI problems," IEEE Trans Neural Syst Rehab, vol. 14, no. 2, pp. 153–159, 2006.*

16. H. Ramoser, J. Muller-Gerking, and G. Pfurtscheller, "Optimal spatial filtering of single trial EEG during imagined hand movement," *IEEE Trans Rehab Eng*, vol. 8, no. 4, pp. 441–446, 2000.
17. B. Blankertz, R. Tomioka, S. Lemm, M. Kawanabe, and K.-R. Müller, "Optimizing spatial filters for robust EEG single-trial analysis," *IEEE Signal Proc Magazine*, vol. 25, no. 1, pp. 41–56, 2008
18. V. Lawhern, A. Solon, N. Waytowich, S. M. Gordon, C. Hung, and B. J. Lance, "EEGNet: A compact convolutional neural network for EEG-based brain–computer interfaces," *J. Neural Eng.*, vol. 15, no. 5, p. 056013, 2018.
19. Zayyanu, Shuaibu & li, qi. (2020). Optimized DNN Classification Framework based on Filter Bank Common Spatial Pattern (FBCSP) for Motor- imagery-based BCI. *International Journal of Computer Applications*. 175. 975-8887. 10.5120/ijca2020920646.

## Supplementary Materials

### Appendix-I

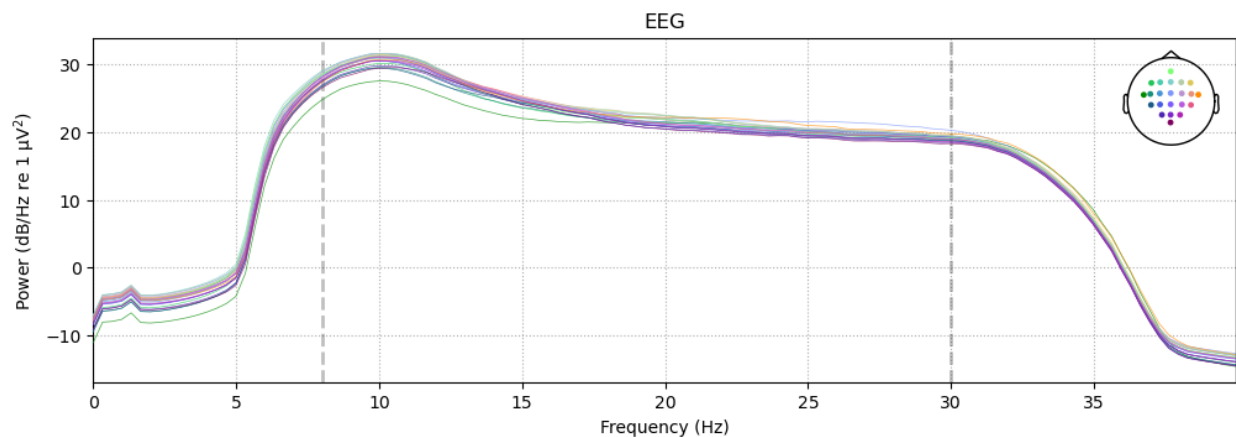


Figure 5. Power spectral density (PSD) of EEG epochs for Subject A02T, averaged across all trials and channels (0–40 Hz). The plot shows dominant spectral power in the alpha (8–12 Hz) and beta (13–30 Hz) frequency ranges, which are critical for motor imagery–related oscillatory dynamics. The topographic plot indicates electrode positions included in the analysis.

### Appendix- II

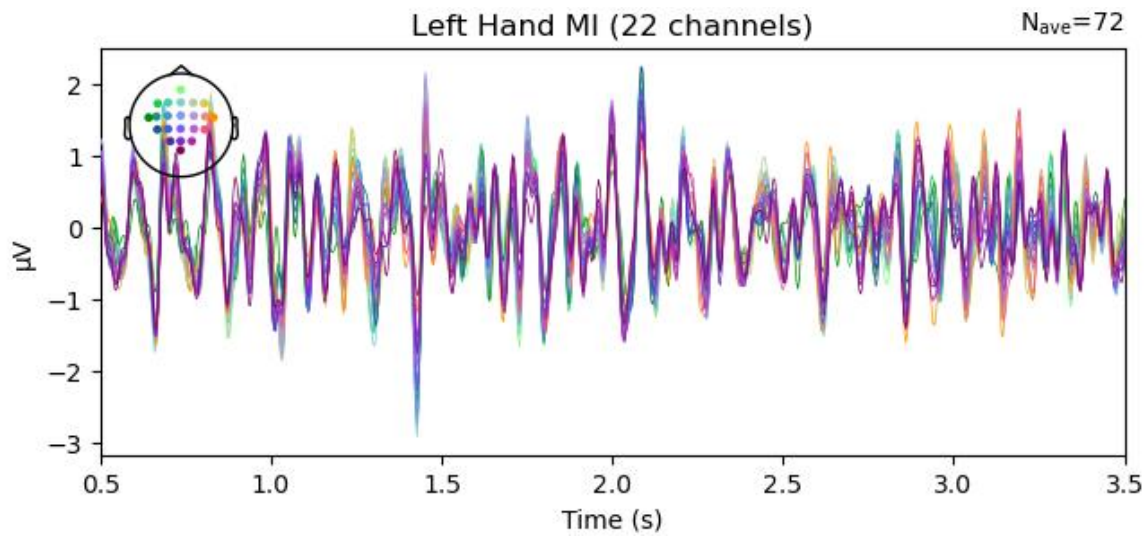


Figure 6. Averaged EEG responses for left-hand motor imagery in Subject A02T, recorded across 22 EEG channels and averaged over 72 trials. The plot illustrates rhythmic oscillatory activity within the 0.5–3.5 s window following cue onset, with amplitudes fluctuating up to  $\pm 3 \mu\text{V}$ . These responses demonstrate consistent motor imagery–related desynchronization and synchronization patterns, confirming that the preprocessing pipeline preserved meaningful neural signatures for subsequent feature extraction and classification.

### Appendix- III

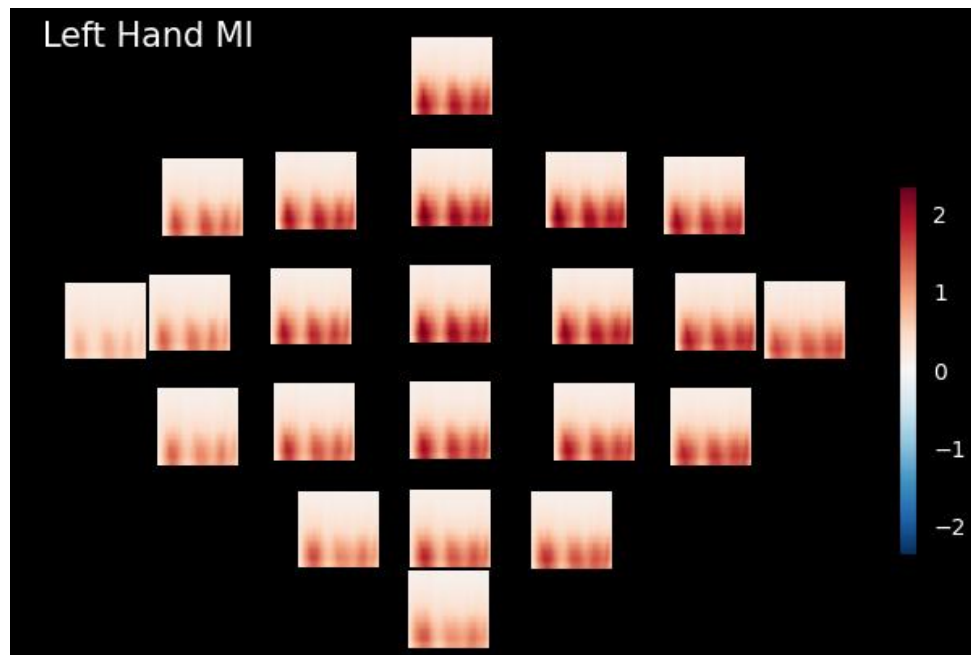


Figure 7. Time–frequency representations (TFRs) of left-hand motor imagery for Subject A02T, computed using the multitaper method across 22 EEG channels. Each subplot corresponds to one channel, showing spectral power changes over time (x-axis) and frequency (y-axis, 8–30 Hz). Warmer colors represent increases in oscillatory power, while cooler colors indicate reductions relative to baseline.